Bull. Mater. Sci., Vol. 32, No. 2, April 2009, pp. 125–133. © Indian Academy of Sciences.

Structural and optical properties of chemically deposited Cd(S–Se) : $CdCl_2$, Sm films

R S SINGH* and S BHUSHAN†

Department of Physics, Pt. Ravishankar Shukla University, Raipur 492 010, India

†Present address: Shri Shankaracharya College of Engineering & Technology, Junwani, Bhilai, Durg 490 006, India

MS received 20 July 2008; revised 19 October 2008

Abstract. **Results of SEM and XRD studies, optical absorption and photoluminescence (PL) emission spectra and photoconductivity (PC), rise and decay studies are reported for Cd(S–Se) : $CdCl_2$, Sm films prepared by chemical deposition method on glass substrates at 60°C in a water bath. SEM studies show ball-type structures along with voids which are related to layered growth. XRD studies show prominent diffraction lines of CdS and CdSe along with some peaks of $CdCl_2$ and impurity Sm. The values of strain (ε), grain size (D) and dislocation density (δ) are evaluated from XRD studies and the nature of crystallinity of the films are discussed. Optical absorption spectra also show the presence of Sm in the lattice. From the results of optical absorption spectra, the band gaps are determined. PL emission spectra of Cd(S–Se) consist of two peaks which are related to the edge emission of CdS and CdSe involving excitons. In Sm-doped emissions corresponding to transitions $^4G_{5/2}$ to $^6H_{5/2}$, $^6H_{7/2}$ and $^6H_{9/2}$ are observed. Sufficiently high photo current (I_{pc}) to dark current (I_{dc}) ratios with a maximum value of the order of 10^6 are also obtained in some special cases. This high photosensitization is related to increase in mobility and life time of carriers due to photo excitation.**

Keywords. **Photoconduction; chemical bath deposition; photoluminescence; energy bandgap.**

1. Introduction

II–VI binary semiconducting compounds, belonging to the cadmium chalcogenide family (CdS, CdSe, CdTe, etc), are considered to be very important materials for a wide spectrum of opto-electronic applications as having specific physical properties such as direct bandgap width and sensitive to infrared part of solar spectrum, good electrical properties (e.g. carrier mobility and life-time) and increased capability in obtaining adjustable n- or p-type conductivity by doping. Particularly, in the visible and near infrared, direct bandgaps of CdSe (1·75 eV) and CdS (2·44 eV), respectively make them candidates for the conversion of low energy light into electricity. Moreover, homogeneous alloys formed over the entire composition range by combination of these compounds allow the production of very interesting ternary $Cd(S_{1-x}–Se_x)$ $(0{\cdot}1 < x < 1)$ system (Murali and Venkatachalam 2008).

Impurities, particularly the rare earth ions when incorporated into a solid, show distinct spectral lines of absorption and emission as a result of the electronic transitions within the $4f^N$ shell configuration (Reisfeld *et al* 2003). The rare-earth ions are characterized by a partially filled $4f$ shell that is well shielded by $5s^2$ and $5p^6$ orbitals. The emission transitions, therefore, yield sharp, near monochromatic lines in the optical spectra. Furthermore, the f–f transitions are fairly insensitive to conditions such as temperature and the surrounding chemical environment (Hufner 1978; Ballato *et al* 1999; Denning 2001). Luminescent properties of rare-earth ions together with a large number of available transitions ranging from the deep ultra violet to the mid infrared make them ideal candidates for optical applications, such as phosphors, lasers, display and amplification systems (Mass *et al* 2002). Particularly, the energy levels of the emitting state of Sm ($^4G_{5/2}$), the impurity selected for the present work ($\sim 19{,}000\ cm^{-1}$) lies below the energy-level of the trap-states in Cd(S–Se) base, hence energy transfer from host defects to the rare-earth activator Sm^{3+} occurs (Frindell *et al* 2003) and hence presents an interesting activator.

Several techniques e.g. vacuum evaporation, spray pyrolysis, molecular beam epitaxy etc (Karanjai and Dasgupta 1987), were employed for the growth of thin films of the ternary system, Cd(S–Se). In this work, Cd(S–Se) films doped with Sm^{3+} ions were deposited by chemical bath deposition method. This is one of the cheapest and simplest techniques for forming films. Chemical deposition techniques for metal chalcogenide semiconductor thin films refer to the deposition of thin films on substrates maintained in contact with dilute chemical bath containing the metal and chalcogen ions (Chopra *et al* 1982). Bhushan and coworkers (Bhushan *et al* 2002, 2006; Bhushan and Pillai 2008) used chemical bath depo-

*Author for correspondence (rss.bhilai@gmail.com)

sition (CBD) technique and reported quite a high photosensitivity, PL, photovoltaic effect and a.c. electroluminescence in such films. The utility of chemical deposition method in metal chalcogenide thin films was reviewed by Mane and Lokhande (2000).

The present paper reports structural and optical properties of Sm^{3+} doped Cd(S–Se) films in terms of SEM, XRD, absorption spectra, PL and PC studies, not explored earlier.

2. Experimental

2.1 *Preparation of films*

Chemical bath deposition technique was used to deposit films of Cd(S–Se) : $CdCl_2$, Sm on glass substrates (cleaned with acetone and double distilled water) of dimension, 24 × 75 mm, by dipping vertically into a mixture of solutions of 1 M cadmium acetate, appropriate ratio of thiourea and sodium selenosulphate [Na_2SeSO_3] solution (prepared by heating elemental selenium (99·9% pure) in aqueous solution of sodium sulphite [Na_2SO_3] at 90°C for 5 h), triethanolamine (TEA) and 30% aqueous ammonia. All the chemicals used were of AR grade. All the solutions were prepared in double distilled water. For preparing doped films, calculated proportions of 0·01 M solutions of samarium nitrate and cadmium chloride were added to the original mixture. After the depositions, the films were cleaned by flushing with distilled water and then dried by keeping the samples in open atmosphere at room temperature.

TEA and ammonia solution were used to adjust pH of the reaction mixture and to increase film adherence. To obtain good quality films, time, temperature of deposition and pH of the solution mixture were optimized. The optimum time, temperature and pH were observed to be 1 h, 60°C and 11·2, respectively. Film thicknesses were determined by optical interference method and were found to lie in the range of 0·4694 ~ 0·4837 μm. Annealing of the films was done at a temperature of 350°C for 3 min.

The mechanism of deposition of CdS films is based on the slow release of Cd^{2+} and S^{2-} ions in aqueous basic solution and subsequent condensation of these ions on the substrates vertically mounted in the solution. The slow release of Cd^{2+} ions is achieved by the dissociation equilibrium of a complex species of cadmium $Cd(TEA)^{2+}$.

$$[(Cd)TEA]^{2+} \leftrightarrow Cd^{2+} + TEA. \quad (1)$$

The S^{2-} ions are provided by the dissociation of thiourea [$SC(NH_2)_2$] in the ammoniacal medium.

$$SC(NH_2)_2 + OH^- \rightarrow CH_2N_2 + H_2O + HS^-, \quad (2)$$

$$HS^- + OH^- \leftrightarrow S^{2-} + H_2O. \quad (3)$$

The hydrolysis of sodium seleno-sulphate (Na_2SeSO_3) in the solution to give Se^{2-} ions is according to the chemical reaction (Ezema and Osuji 2007)

$$Na_2SeSO_3 + OH^- \leftrightarrow Na_2SO_4 + HSe^-, \quad (4)$$

$$HSe^- + OH^- \leftrightarrow H_2O + Se^{2-}. \quad (5)$$

Similarly, the hydrolysis of ammonia in water to give OH^- ion is according to the equation

$$NH_3 + H_2O \leftrightarrow NH_4^+ + OH^-. \quad (6)$$

When ammonia is added to the Cd^{2+} salt solution, $Cd(OH)_2$ starts precipitating, when the solubility-product of $Cd(OH)_2$ is exceeded.

$$Cd^{2+} + 2OH^- \leftrightarrow Cd(OH)_2. \quad (7)$$

The $Cd(OH)_2$ precipitate dissolves in excess ammonia solution to form the complex cadmium tetra-amine ions, $[Cd(NH_3)_4]^{2+}$.

$$Cd^{2+} + 4NH_3 \leftrightarrow [Cd(NH_3)_4]^{2+}. \quad (8)$$

Finally, the deposition of Cd(S–Se) thin film occurs according to the following reaction, when the ionic-product of Cd^{2+} and S^{2-} or Cd^{2+} and Se^{2-} ions in the solutions controls the rate of precipitation and hence the rate of film formation (Kale and Lokhande 2004).

$$[Cd(NH_3)_4]^{2+} + S^{2-} + Se^{2-} \leftrightarrow Cd(S–Se) + 4NH_3. \quad (9)$$

The role of $CdCl_2$ in the film formation is two-fold: (i) it helps in re-crystallization of the base material and (ii) it acts as a flux for incorporation of impurity in the base material.

The growth mechanism of thin films using chemical bath deposition (CBD) method can take place either in the bulk of the solution (homogeneous precipitation process) or at the substrate surface (heterogeneous process). It can be considered as 'cluster by cluster' growth, leading to the particulate films. The latter is a growth mechanism involving the reaction of atomic species at the surface, it corresponds to an atom by atom process, also called 'ion by ion' process (Kaur *et al* 1980).

2.2 *PL and PC cells*

The PL cell consisted of the film deposited on the substrates. For PC studies, coplanar electrodes (1·5 mm wide and 24 mm long at a separation of 2 mm) were formed by applying colloidal silver paint to the surface of the film. The photocurrents were measured by exposing the total area of the film.

3. Results and discussion

3.1 *SEM studies*

The SEM micrograph of Cd(S–Se) : $CdCl_2$, Sm films chemically deposited on glass substrate at 60°C in WB

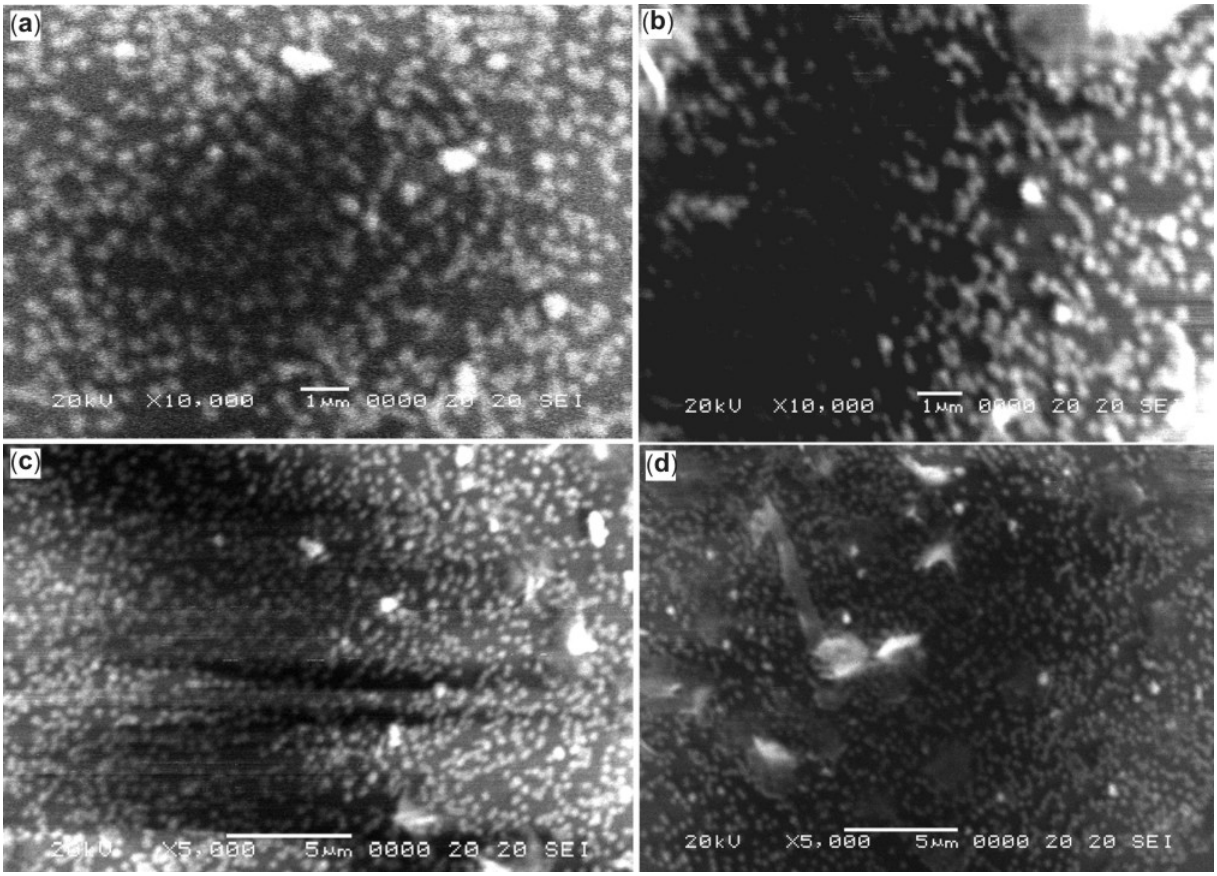

Figure 1. SEM micrographs of (**a**) unannealed $Cd(S_{0.95}–Se_{0.05}) : CdCl_2$ (3 ml), Sm (3 ml) film, (**b**) unannealed $Cd(S_{0.7}–Se_{0.3})$: $CdCl_2$ (2 ml), Sm (2 ml) film, (**c**) annealed $Cd(S_{0.95}–Se_{0.05})$: $CdCl_2$ (3 ml), Sm (3 ml) film and (**d**) annealed $Cd(S_{0.7}–Se_{0.3})$: $CdCl_2$ (2 ml), Sm (2 ml) film.

and their annealed samples are presented in figures 1(a), (b), (c) and (d), respectively. Ball-type structure along with some voids are observed. This kind of structure probably appears due to layered type growth of the material, which under continued deposition forms such structure due to turning followed by overlap of different layers.

3.2 *XRD studies*

The X-ray diffractograms of Cd(S–Se) : $CdCl_2$, Sm films chemically deposited on glass substrate at 60°C in WB and their annealed samples are presented in figures 2(a), (b), (c) and (d), respectively. The corresponding data are presented in table 1.

The assignments of peaks were made by comparing with ASTM data, and calculation of lattice constants and their comparison with the reported values. The different assigned peaks are mentioned in the figures. Thus, prominent peaks of CdS [$(111)_c$, $(101)_h$, $(200)_c$, $(220)_c$, $(112)_h$ and $(102)_h$] and CdSe [$(100)_h$, $(002)_h$ and $(110)_h$] along with two peaks of Sm [$(101)_h$ and $(104)_h$] and one peak of $CdCl_2$ [$(021)_h$] are observed. The intensities of $(111)_c$ peak of CdS and $(100)_h$ peak of CdSe are dominant. Existence of Sm and $CdCl_2$ are also found.

Different layers of CdS are observed in cubic as well as hexagonal phases. The formation of the hexagonal and cubic phases are known to be created through different arrangements of atomic layers. The hexagonal phase consists of the sequence of atomic layers defined as *ABABAB*----- and that of cubic in *ABCABCABC*----- (Kittel 1995). It is also possible to find mixed forms with random stacking of very long period repeats as is found in polytypes of SiC (Ibach and Lüth 1991). The total crystal consists of different atomic layers of CdS in cubic as well as hexagonal phases along with some atomic layers of CdSe in hexagonal phases. According to Langer *et al* (1996), one might think of solid solutions as mixtures of microcrystalline regions of the pure CdSe and CdS, where each microregion might consist of a number of unit cells of each material with the lattice-constant of CdS stressed by surrounding CdSe and that of CdSe compressed by its CdS neighbours. Such a model can explain uniform shift of absorption edge with variation in composition. A possibility of solid solution consisting of statistical distribution of CdSe and CdS with respect to their

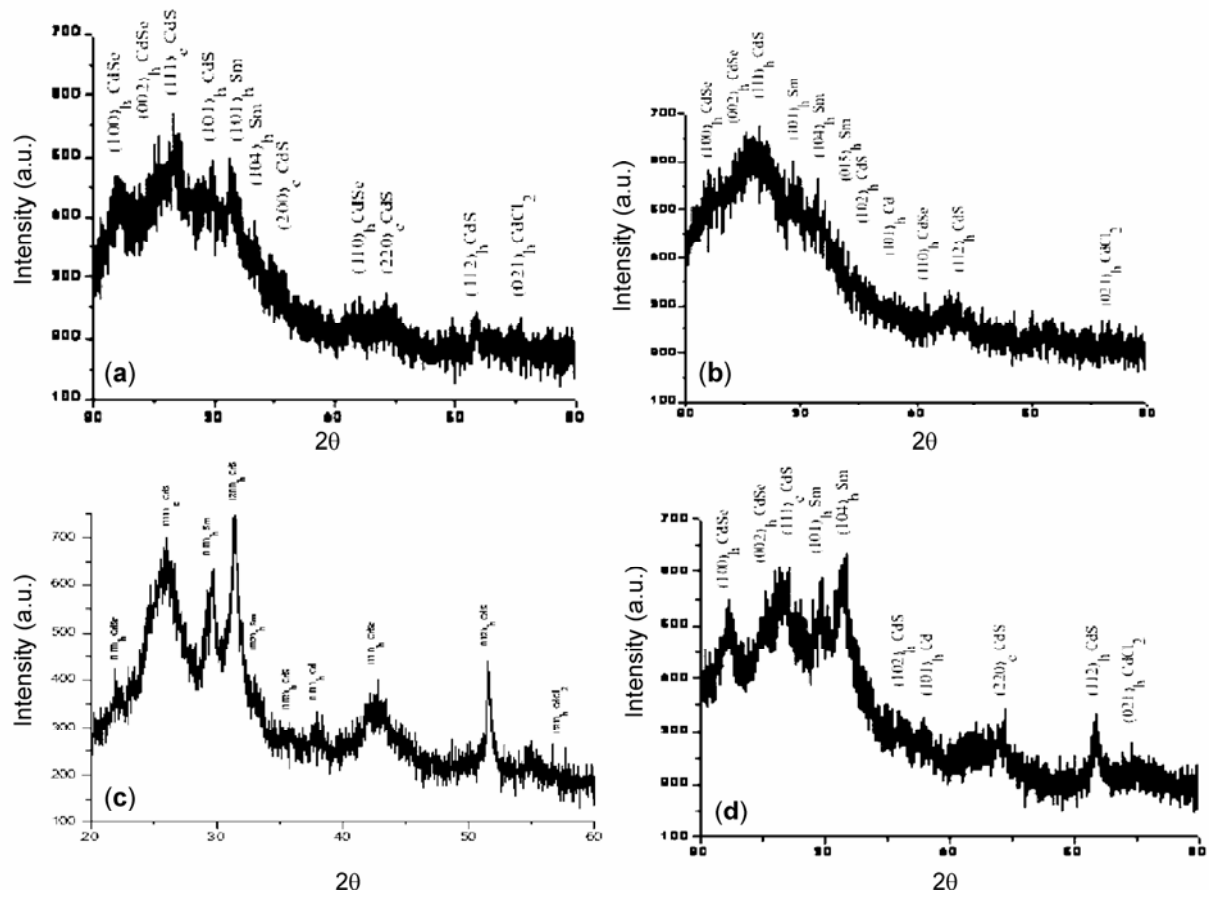

Figure 2. X-ray diffractograms of (**a**) unannealed $Cd(S_{0.95}–Se_{0.05}) : CdCl_2$ (3 ml), Sm (3 ml) film, (**b**) unannealed $Cd(S_{0.7}–Se_{0.3}) : CdCl_2$ (2 ml), Sm (2 ml) film, (**c**) annealed $Cd(S_{0.95}–Se_{0.05}) : CdCl_2$ (3 ml), Sm (3 ml) film and (**d**) annealed $Cd(S_{0.7}–Se_{0.3}) : CdCl_2$ (2 ml), Sm (2 ml) film.

overall concentration was also mentioned by these workers. It should be noted that shift of absorption edge has already been observed in the present case.

The particle size, D (Wilson 1963), strain value, ε (Senthilkumar *et al* 2005) and dislocation density, δ (Williamson and Smallman 1956) were obtained for (111)c peak of CdS by using the well known formulae and corresponding values are listed in table 2. It is noticed that with annealing of films, FWHM, strain value and dislocation density decrease, whereas the particle size increases. The decrease in dislocation density suggests that films become more crystalline. Annealing of thin films increases the grain size resulting in better crystallinity.

3.3 *Optical absorption spectra*

The optical absorption measurements of the Sm-doped Cd(S–Se) films were carried out at room temperature by placing an uncoated identical glass substrate in the reference beam. The optical spectra of the films were recorded in the wavelength range 300–700 nm. The energy band gaps of the materials in these films were determined from the absorption spectra.

The optical absorption spectra of CdS and different Cd(S–Se) films prepared on glass substrates are shown in figure 3. Bandgaps were determined from the extrapolation of the plots between $(\alpha h\nu)^2$ vs $h\nu$ (Tauc's plots) (figure 4). It is found that with increase in concentration of CdSe the bandgap decreases: [$Cd(S_{0.95}–Se_{0.05})$: 2·36 eV; $Cd(S_{0.9}–Se_{0.1})$: 2·33 eV; $Cd(S_{0.8}–Se_{0.2})$: 2·26 eV; $Cd(S_{0.7}–Se_{0.3})$: 2·19 eV; $Cd(S_{0.6}–Se_{0.4})$: 2·12 eV]. A plot of E_g vs CdS/CdSe ratio is shown in figure 5. This shows that a common lattice of Cd(S–Se) is formed through the solid solution formation. Slight changes in bandgaps are observed in presence of $CdCl_2$ and Sm. The overall absorption in presence of Se and Sm decreases which shows that the films become more transparent in their presence. The spikes observed at around 300 nm may also occur due to nanocrystalline effects under which the continuum of states in conduction band (CB) and valence band (VB) are broken into discrete states (Efros and Efros 1982).

Table 1. XRD data of different chemically deposited Cd(S–Se) : $CdCl_2$, Sm films on glass substrate at 60°C in WB.

d-values		Relative intensities			Lattice-constants (Å)	
Obs.	Rep.	Obs.	Rep.	*hkl*	Obs.	Rep.
(a) $Cd(S_{0.95}–Se_{0.05}) : CdCl_2$, Sm (3 ml)						
3·7245	3·7239	91·3	100	$(100)_h$ CdSe	a = 4·3	a = 4·3, c = 7·02
3·5010	3·51	93·2	65·85	$(002)_h$ CdSe	a = 4·3, c = 7·002	a = 4·3, c = 7·02
3·3609	3·36	100	100	$(111)_c$ CdS	a = 5·786	a = 5·818
3·181	3·16	86·2	100	$(101)_h$ CdS	a = 4·102, c = 6·5633	a = 4·135, c = 6·71
3·0919	3·09	86·9	30	$(101)_h$ Sm		
2·8173	2·81	82·5	40	$(104)_h$ Sm		
2·9015	2·9	69·05	40	$(200)_c$ CdS	a = 5·803	a = 5·818
2·1542	2·15	45·5	82·43	$(110)_h$ CdSe	a = 4·3084	a = 4·3, c = 7·02
2·0404	2·06	47·7	57	$(220)_c$ CdS	a = 5·776	a = 5·818
1·7616	1·76	42·5	45	$(112)_h$ CdS	a = 4·13, c = 6·758	a = 4·135, c = 6·71
1·658	1·658	40·73	12	$(021)_h$ $CdCl_2$	a = 3·851, c = 17·98	a = 3·84, c = 17·49
(b) $Cd(S_{0.7}–Se_{0.3}) : CdCl_2$, Sm (2 ml)						
3·7227	3·7239	91·74	100	$(100)_h$ CdSe	a = 4·2986	a = 4·3, c = 7·02
3·5224	3·52	98·08	65·85	$(002)_h$ CdSe	a = 4·2986, c = 7·0448	a = 4·3, c = 7·02
3·3685	3·36	100	100	$(111)_c$ CdS	a = 5·834	a = 5·818
3·0999	3·09	88·79	30	$(101)_h$ Sm		
2·8283	2·81	83·33	40	$(104)_h$ Sm		
2·6905	2·68	76·69	40	$(015)_h$ Sm		
2·4601	2·4502	56·49	25	$(102)_h$ CdS	a = 4·146, c = 6·723	a = 4·135, c = 6·71
2·3194	2·345	47·19	100	$(101)_h$ Cd	a = 2·989, c = 5·569	a = 2·974, c = 5·62
2·1705	2·15	44·54	82·43	$(110)_h$ CdSe	a = 4·304, c = 7·045	a = 4·3, c = 7·02
1·7757	1·76	39·08	45	$(112)_h$ CdS	a = 4·118, c = 6·78	a = 4·135, c = 6·71
1·659	1·658	38·05	12	$(021)_h$ $CdCl_2$	a = 3·853, c = 17·90	a = 3·84, c = 17·49
(c) $Cd(S_{0.95}–Se_{0.05}) : CdCl_2$, Sm (3 ml) (annealed)						
3·7294	3·7239	52·17	100	$(100)_h$ CdSe	a = 4·3063	a = 4·3, c = 7·02
3·335	3·36	94·85	100	$(111)_c$ CdS	a = 5·776	a = 5·818
3·094	3·09	85·77	30	$(101)_c$ Sm		
2·94	2·9	100	40	$(200)_h$ CdS	a = 5·88	a = 5·818
2·70	2·68	55·96	40	$(015)_c$ Sm		
2·4587	2·4502	40·37	25	$(102)_h$ CdS	a = 4·142, c = 6·721	a = 4·135, c = 6·71
2·315	2·345	42	100	$(101)_h$ Cd	a = 2·945, c = 5·573	a = 2·974, c = 5·62
2·154	2·15	50·54	82·43	$(110)_h$ CdSe	a = 4·308, c = 7·047	a = 4·3, c = 7·02
1·766	1·76	56·50	45	$(112)_h$ CdS	a = 4·126, c = 6·75	a = 4·135, c = 6·71
1·660	1·658	34·82	12	$(021)_h$ $CdCl_2$	a = 3·849, c = 17·81	a = 3·84, c = 17·49
(d) $Cd(S_{0.7}–Se_{0.3}) : CdCl_2$, Sm (2 ml) (annealed)						
3·7274	3·7239	88	100	$(100)_h$ CdSe	a = 4·3048	a = 4·3, c = 7·02
3·54	3·51	90·4	65·85	$(002)_h$ CdSe	a = 4·3040, c = 7·08	a = 4·3, c = 7·02
3·333	3·51	97·6	100	$(111)_c$ CdS	a = 5·773	a = 5·818
3·091	3·09	94·4	30	$(101)_c$ Sm		
2·84	2·81	100	40	$(104)_h$ Sm		
2·456	2·4502	50·72	25	$(102)_h$ CdS	a = 4·139, c = 6·719	a = 4·135, c = 6·71
2·317	2·345	51·2	100	$(101)_h$ Cd	a = 2·984, c = 5·622	a = 2·974, c = 5·62
2·054	2·058	48·8	80	$(220)_c$ CdS	a = 5·8096	a = 5·818
1·764	1·76	53·12	45	$(112)_h$ CdS	a = 4·14, c = 6·715	a = 4·135, c = 6·71
1·661	1·658	34·4	12	$(021)_h$ $CdCl_2$	a = 3·851, c = 17·91	a = 3·84, c = 17·49

Also, in Sm-doped film, a weak absorption peak is observed at around 404 nm. Li *et al* (2007) had observed strong PL excitation at 404 nm wavelength in his Sm^{3+} doped sample, which was attributed to the transition from the lower level $^6H_{5/2}$ of Sm^{3+} to the higher level $^4K_{11/2}$. In the PL emission spectrum of Sm^{3+}, three peaks in the orange-red region near 563, 595 and 641 nm were observed, which were assigned to the intra-4*f*-shell transitions from the excited level $^4G_{5/2}$ to the lower levels $^6H_{5/2}$, $^6H_{7/2}$ and $^6H_{9/2}$, respectively.

3.4 *PL emission spectra*

Maximum PL emission is observed for 0·7 : 0·3 combination of CdS : CdSe and hence this combination was used

Table 2. Values of FWHM, particle size, strain and dislocation density corresponding to $(111)_c$ peak of CdS for different chemically deposited Cd(S–Se) : $CdCl_2$, Sm films on glass substrate at 60°C in WB.

Sample	FWHM, β (radian)	Particle size, D (nm)	Strain, ε (lin^{-2}/m^{-4})	Dislocation density, δ ($\times 10^{15}$ lin/m^2)
$Cd(S_{0.95}–Se_{0.05})$: $CdCl_2$, Sm (3 ml)	0·2282	6·5254	0·00555	2·34847
$Cd(S_{0.7}–Se_{0.3})$: $CdCl_2$, Sm (2 ml)	0·2796	5·3060	0·006828	3·55192
$Cd(S_{0.95}–Se_{0.05})$: $CdCl_2$, Sm (3 ml) (annealed)	0·1630	9·1545	0·003958	1·19325
$Cd(S_{0.7}–Se_{0.3})$: $CdCl_2$, Sm (2 ml) (annealed)	0·2326	6·3874	0·005673	2·45105

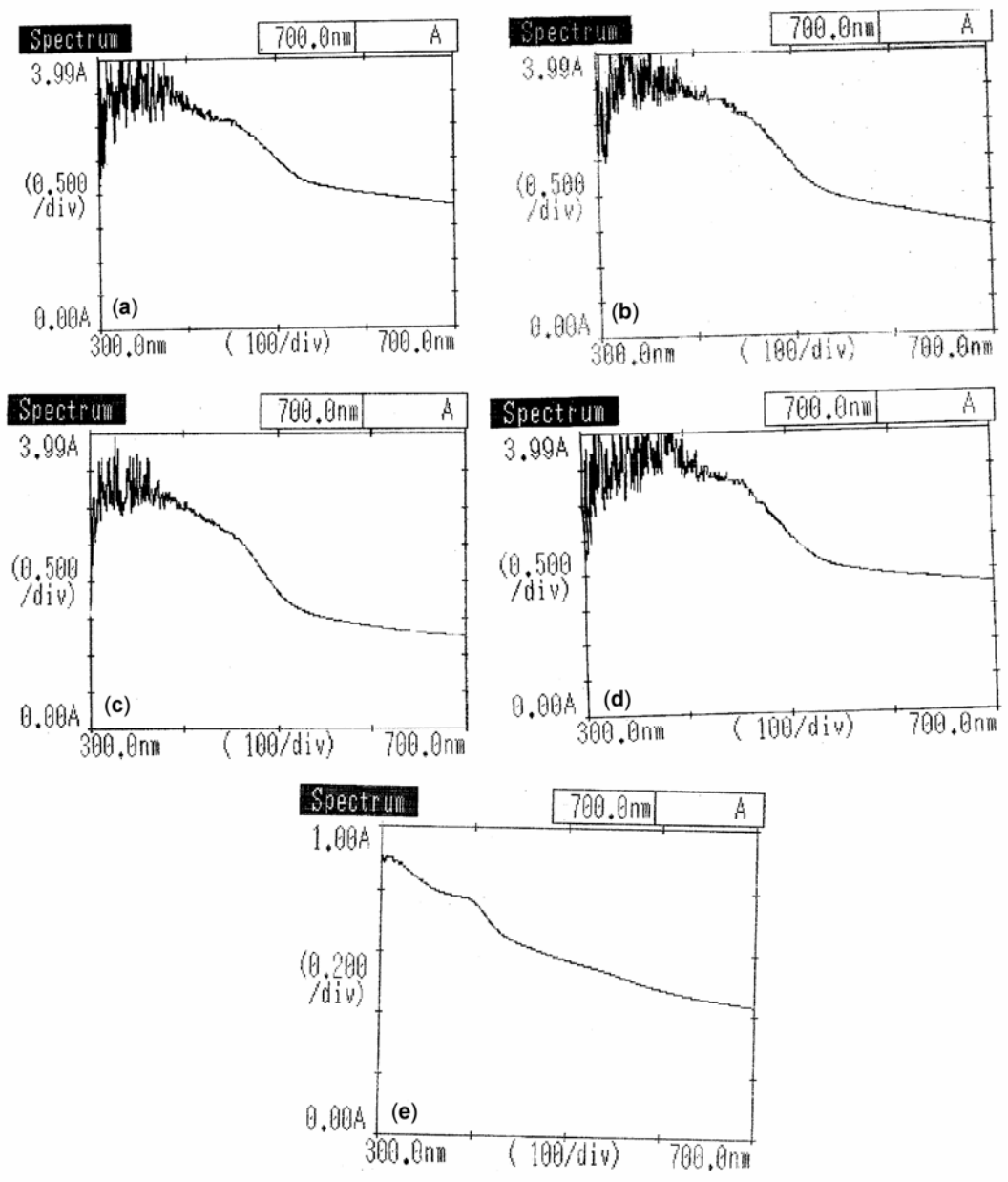

Figure 3. Absorption spectra of (**a**) CdS-film, (**b**) $Cd(S_{0.95}–Se_{0.05})$ film, (**c**) $Cd(S_{0.95}–Se_{0.05})$: $CdCl_2$ (3 ml) film, (**d**) $Cd(S_{0.95}–Se_{0.05})$: $CdCl_2$ (3 ml), Sm (3 ml) film and (**e**) $Cd(S_{0.7}–Se_{0.3})$: $CdCl_2$ (2 ml), Sm (2 ml) film.

for PL studies. In the presence of flux, at its different concentrations, the highest emission appears at a volume of 2 ml $CdCl_2$. Therefore, this concentration was used in the presence of impurities. Plots of PL intensity vs wavelength for CdS and different Cd(S–Se) films are shown in figures 6(a) and (b), respectively; and those for varying

volumes of Sm^{3+} are shown in figure 7. The corresponding peak positions are mentioned in table 3.

PL emission spectrum of CdS was found to consist of a peak at 511 nm. This emission is quite close to the band-gap as obtained from the absorption spectrum. Thus, this may be due to the edge emission of CdS. This edge emission was attributed to the excitonic transitions involving free excitons (Thomas and Hopfield 1962). The peak positions of emission spectra of CdS and Cd(S–Se) are presented in table 3. The peak positions in Cd(S–Se) at different compositions of S and Se were obtained by deconvolution into Gaussian curves and for one composition, these peaks are shown in figure 8. The peak observed at 516 nm for $Cd(S_{0.95}–Se_{0.05})$ shows a shift towards higher wavelength with increasing concentration of Se. This emission, thus, can be identified as the edge emission of Cd(S–Se). Owing to similar excitonic nature in both CdS and CdSe, this emission can be attributed to the radiative decay of the free exciton. The peak at 494 nm may be attributed to the exciton bound to neutral donor levels formed by sulphur/excess Cd (Bhushan and Oudhia 2008). Higher volumes of sodium seleno sulphate (Na_2SeSO_3) were added for increasing the concentration of CdSe. Thus, the formation of more sulphur could be expected, enhancing the emission in its presence (Bhushan and Oudhia 2008). A prominent peak at 505 nm in Cd-rich single crystals of CdS at room temperature was also reported earlier (Kokubun and Kaeriyama 1975).

Table 3. Values of peak positions of CdS and different chemically deposited Cd(S–Se) films on glass substrate at 60°C in WB.

Systems	Peak positions
CdS	511
$Cd(S_{0.95}–Se_{0.05})$	494, 516
$Cd(S_{0.9}–Se_{0.1})$	494, 525
$Cd(S_{0.8}–Se_{0.2})$	494, 542
$Cd(S_{0.7}–Se_{0.3})$	494, 559
$Cd(S_{0.6}–Se_{0.4})$	494, 577
$Cd(S_{0.7}–Se_{0.3})$: $CdCl_2$ (2 ml), Sm (2 ml)	563, 595, 614

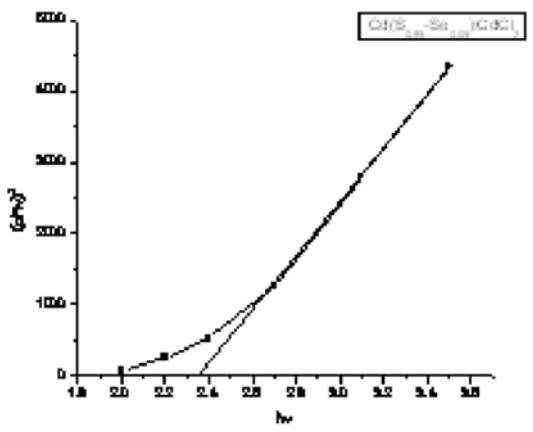

Figure 4. Tauc's plot for unannealed Cd ($S_{0.95}–Se_{0.05}$) film.

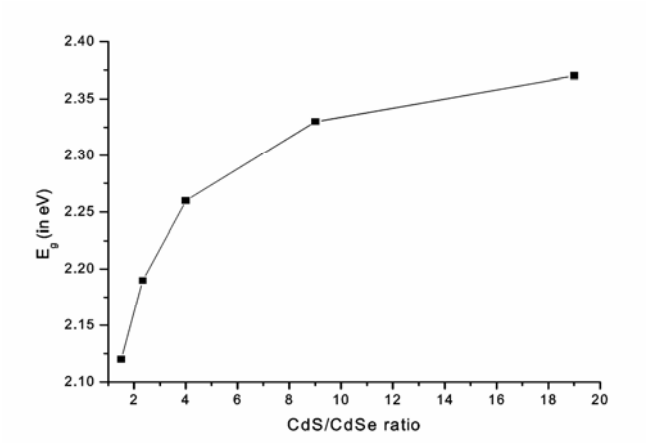

Figure 5. Plot of variation of energy-gap (E_g) vs CdS/CdSe ratio.

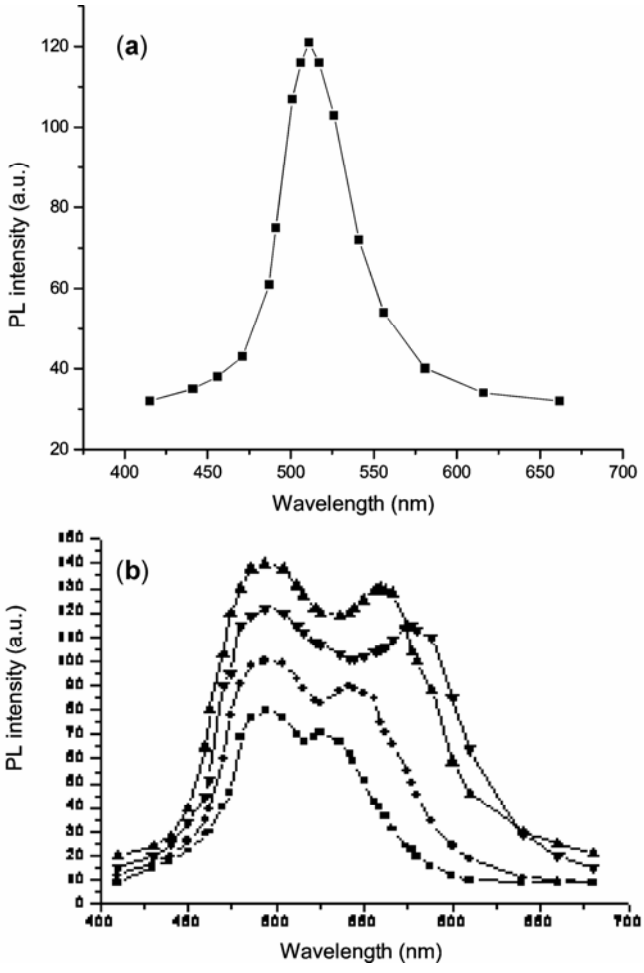

Figure 6. PL emission spectra of (**a**) CdS and (**b**) different $Cd(S_{1-x}–Se_x)$ films prepared at 60°C with different values of *x*: ■ $Cd(S_{0.9}–Se_{0.1})$, ● $Cd(S_{0.8}–Se_{0.2})$, ▲ $Cd(S_{0.7}–Se_{0.3})$ and ▼ $Cd(S_{0.6}–Se_{0.4})$.

Table 4. Values of I_{dc}, I_{pc}, I_{pc}/I_{dc}, lifetime (τ), mobility (μ) and trap depth (E) for different Cd(S–Se) films. (Temp. of preparation = 60°C; duration = 1 h).

Sample	I_{pc} (nA)	I_{pc} (μA)	Gain (I_{pc}/I_{dc})	Lifetime, τ (s)	Mobility, μ (cm^2/Vs)	Trap depth (eV)
$Cd(S_{0.95}–Se_{0.05})$	0·2	134	$6·7 \times 10^5$	39·41	45·33	$E_1 = 0·673$, $E_2 = 0·665$
$Cd(S_{0.95}–Se_{0.05}) : CdCl_2$	0·1	264	$2·64 \times 10^6$	48·01	93·33	$E_1 = 0·684$, $E_2 = 0·668$
$Cd(S_{0.95}–Se_{0.05}) : CdCl_2$; Sm at 60°C in WB	0·05	402·41	$8·05 \times 10^6$	61·9	148·19	$E_1 = 0·696$, $E_2 = 0·679$
$Cd(S_{0.95}–Se_{0.05}) : CdCl_2$; Sm at 60°C in WB (annealed)	~0	54·2	Very high	67·4	Very high	$E_1 = 0·699$, $E_2 = 0·681$

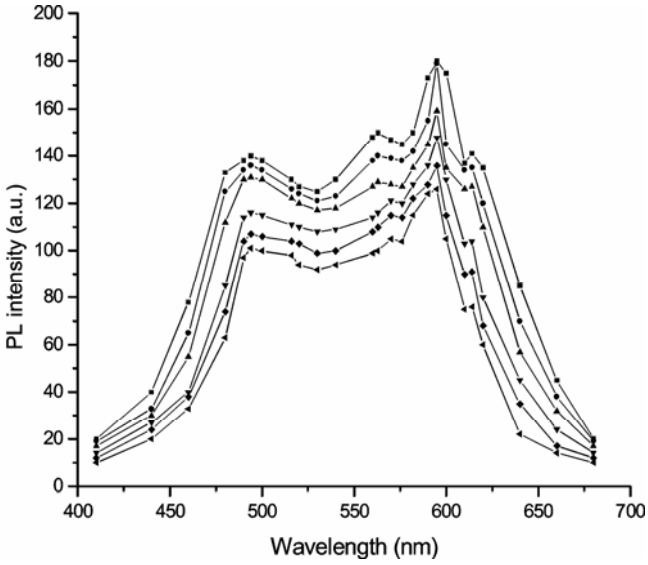

Figure 7. PL emission spectra of $Cd(S_{0·7}–Se_{0·3}) : CdCl_2$ (2 ml), Sm (2 ml) films prepared on glass substrates at 60°C at different volumes of $Sm(NO_3)_3$ (0·01 M): ■ 2 ml, ● 4 ml, ▲ 6 ml, ▼ 8 ml, ◆ 10 ml and ◀ 12 ml.

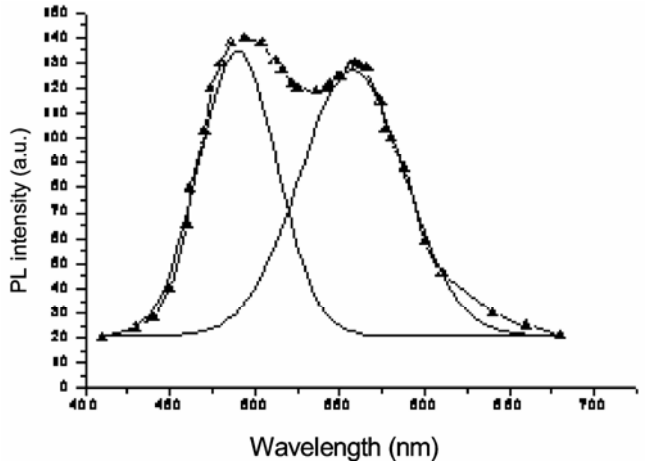

Figure 8. Deconvolution of PL emission spectrum of $Cd(S_{0·7}–Se_{0·3})$ into Gaussian curves.

Further, the possibility of shift of emission peak due to nanocrystalline effect cannot be ignored. Thus, the 494 nm peak may be due to the shift of bulk emission of CdS at 511 nm and the 559 nm peak may be due to the shift in peak position of CdSe at 712 nm. In presence of Sm, along with the peak at 494 nm, other peaks observed are at 563 nm, 595 nm and 614 nm, respectively. These peaks may be associated to the transitions from the excited level $^4G_{5/2}$ to ground levels $^6H_{5/2}$, $^6H_{7/2}$ and $^6H_{9/2}$, respectively $\{^4G_{5/2} \rightarrow {}^6H_{5/2}$, $^4G_{5/2} \rightarrow {}^6H_{7/2}$ and $^4G_{5/2} \rightarrow {}^6H_{9/2}\}$ (figure 9).

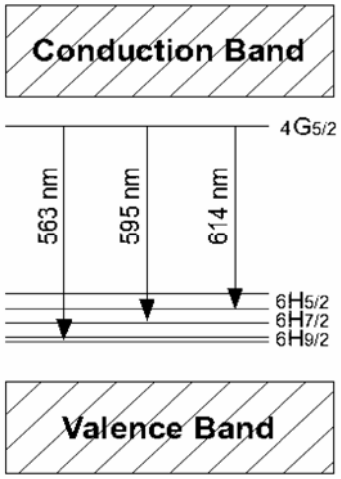

Figure 9. Schematic diagram showing various emission transitions in $Cd(S_{0·7}–Se_{0·3}) : CdCl_2$ (2 ml), Sm (2 ml) films.

3.5 *PC rise and decay studies*

The PC rise and decay curves of different Cd(S–Se) films prepared on glass substrates are shown in figure 10. It is observed that when light is illuminated on the film, the photocurrent first increases rapidly due to generation of *e–h* pairs through absorption of photons by the materials of the films mostly from the surface region of the film. The rate of increase of photocurrent decreases with time due to recombination of carriers and after some time, the photocurrent is almost constant due to a balance between the generation and recombination i.e. resulting in saturated value of current. When light is turned off, photocurrent decreases very rapidly and after a few seconds, it decreases steadily with respect to time. Here surface recombination is very high and it leads to a lower carrier concentration at the surface. The system tends to its initial stage by relaxation process, which gives low and steady decay of photocurrent.

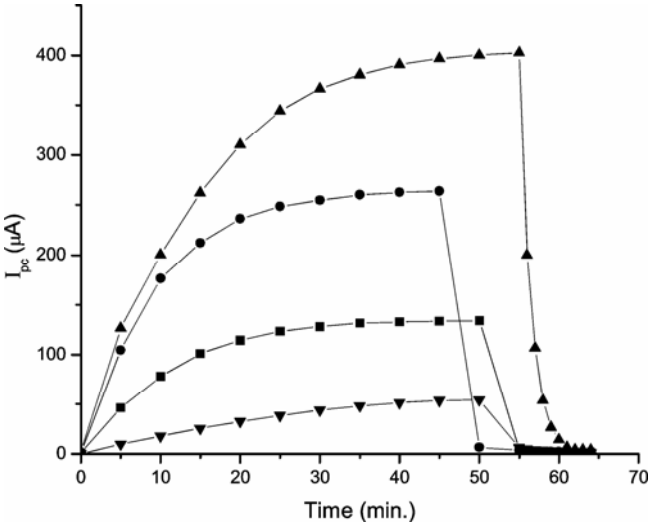

Figure 10. PC rise and decay curves of different Cd(S–Se) films prepared on glass substrates at 60°C: ■ $Cd(S_{0·95}–Se_{0·05})$, ● $Cd(S_{0·95}–Se_{0·05}) : CdCl_2$, ▲ $Cd(S_{0·95}–Se_{0·05}) : CdCl_2$, Sm (3 ml) and ▼ annealed $Cd(S_{0·95}–Se_{0·05})$: $CdCl_2$, Sm (3 ml).

Maximum photocurrent was observed in the case of 0·95 : 0·05 combination of CdS to CdSe. In the presence of $CdCl_2$, the maximum current was observed for a volume of 3 ml (0·001 M). The values of I_{pc}/I_{dc} ratio, trap-depths, instantaneous lifetime and mobility were evaluated by methods described in earlier publications (Bhushan *et al* 2001) and the corresponding values for the different cases are summarized in table 4.

It is observed that the values of lifetime and mobility both increase in the presence of impurities, which accounts for the better photo-response.

4. Conclusions

SEM studies of the chemically deposited Sm-doped Cd(S–Se) films show ball-type structures, which may be due to layered growth. X-ray diffractograms of Cd (S–Se) : $CdCl_2$, Sm films show the presence of CdS and CdSe along with some peaks of $CdCl_2$ and Sm. From the calculation of strain and dislocation density, crystallinity is found to be better in RT preparation. PL emission spectra of the doped films consist of peaks due to transitions in impurity levels. PC rise and decay studies show I_{pc}/I_{dc} ratio of the order of 10^6. Such higher photosensitization occurs due to increase in life-time and mobility of carriers.

Acknowledgements

The authors are grateful to IUC-DAE, Indore, for giving consent for completing SEM and XRD studies at the consortium. One of the authors (RSS) is thankful to the University Grants Commission, New Delhi, for the award of a Teacher Fellowship under 10th plan.

References

Ballato J, Lewis J S and Holloway P 1999 *M.R.S. Bull.* **24** 51

Bhushan S and Oudhia A 2008 *Optoelectron. Rev.* (*Romania*) (accepted)

Bhushan S and Pillai S 2008 *Rad. Eff. Def. Sol.* **163** 241

Bhushan S, Mukherjee M and Bose P 2001 *Radiat. Eff. & Def. Solids* **153** 367

Bhushan S, Mukherjee M and Bose P 2002 *J. Mater. Sci.* **13** 581

Bhushan S, Shrivastava S and Shrivastava A 2006 *J. Mater. Sci.* **41** 7483

Chopra K L, Kaintela R C, Pandya D R and Thakoor A P 1982 *Physics of thin films* (eds) G Hass *et al* (New York: Academic Press) **12** p. 201

Denning R G 2001 *J. Mater. Chem.* **11** 19

Efros A L and Efros A L 1982 *Sov. Phys. Semicond.* **16** 722

Ezema F I and Osuji R U 2007 *Chalcogenide Letts* **4** 69

Frindell K L, Bartl M H, Robinson M R, Bazan G C, Popitsch A and Stucky G D 2003 *J. Solid State Chem.* **172** 81

Hufner S 1978 *Optical spectra of transparent rare earth compounds* (New York: Academic Press)

Ibach Herald and Lüth Hans 1991 *Solid state physics* (*An introduction to theory and experiment*) (Springer International Student Edition) p. 25

Kale R B and Lokhande C D 2004 *Appl. Surf. Sci.* **223** 343

Karanjai M K and Dasgupta D 1987 *Thin Solid Films* **150** 309

Kaur I, Pandya D K and Chopra K L 1980 *J. Electrochem. Soc.* **127** 943

Kittel C 1995 *Introduction to solid state physics* (New York: John Wiley & Sons) 7th ed. p. 18

Kokubun V and Kaeriyama T 1975 *J. Appl. Phys.* (*Japan*) **14** 1403

Langer D W, Park Y S and Euwama R N 1996 *Phys. Rev.* **152** 788

Li Yu-Chun, Chang Yen-Hwei, Lin Yu-Feng, Chang Yee-Shin and Lin Yi-Jing 2007 *J. Alloys & Compounds* **439** 367

Mane R S and Lokhande C 2000 *Mater. Chem. Phys.* **65** 1

Mass H, Currao A and Calzaferri G 2002 *Angew. Chem. Int. Ed.* **41** 2495

Murali K R and Venkatachalam K 2008 *Chalcogenide Letts* **5** 181

Reisfeld R, Saraidarov T, Ziganski E, Gaft M, Lis S and Pietraszkiewiez M 2003 *J. Lumin.* **243** 102

Senthilkumar V, Venketachalam S, Vishwanatham C, Gopal S, Narayandass S K, Mangalraj B, Wilson K C and Vijaykumar V 2005 *Cryst. Res. Technol.* **40** 573

Thomas D G and Hopfield J J 1962 *Phys. Rev.* **128** 2135

Williamson G B and Smallman R C 1956 *Philos. Mag.* **1** 34

Wilson A P J 1963 *Mathematical theory of X-ray powder diffractometry* (New York: Gordon and Breach) p. 62